

REVIEW ARTICLE

Novel Cardiac SPECT Technology with Semiconductor Detectors: Emerging Trends and Future Perspective

Masao Miyagawa, MD, PhD¹⁾, Yoshiko Nishiyama, MD, PhD¹⁾, Rami Tashiro, MD, PhD¹⁾, Hayato Ishimura RT¹⁾, Yasuyuki Takahashi, PhD²⁾, Teruhito Mochizuki, MD, PhD¹⁾

Received: June 26, 2015/Revised manuscript received: July 20, 2015/Accepted: July 24, 2015

© The Japanese Society of Nuclear Cardiology 2015

Abstract

Recently, two vendors have introduced novel SPECT scanners with solid-state semiconductor detectors: Discovery NM530c (D530c) and D-SPECT utilizing the same cadmium zinc-telluride (CZT) detectors, with a different combination of high-sensitivity multi-pinhole or parallel-hole collimator which focuses on the myocardium. The physical performance is dramatically higher than that of conventional Anger cameras, however, 2 CZT cameras are inherently different. Spatial resolution and contrast-to-noise ratio are better with the D530c, whereas detection sensitivity is higher with the D-SPECT. Although ^{99m}Tc-labeled myocardial perfusion tracers might not be ideal, estimation of absolute myocardial blood flow or coronary flow reserve using dynamic CZT SPECT is of great interest and a challenging subject.

Keywords: Myocardial perfusion imaging, Cadmium zinc telluride, Cardiac SPECT, Coronary flow reserve, Effective dose, Dynamic imaging

Ann Nucl Cardiol 2015 ; 1 (1) : 18-26

Over the past 40 years, radionuclide myocardial perfusion imaging (MPI) has become a major tool in the noninvasive evaluation of coronary artery disease (CAD). Whereas in 1990, fewer than 3 million nuclear cardiology studies were performed in the USA, the overall procedural utilization for stress MPI reached its height in 2006 with over 10 million studies and Medicare payment over 1 billion dollars (1). After the dramatic increase at a rate of often greater than 20% per year (2), however, a reduction in MPI use had begun in 2007 which continued through 2011 and declined by 51%. These reductions could not only be explained by increasing use of alternative modalities such as coronary CT angiography but there were several concerns about its overutilization. The National Council on Radiation Protection and Measurements reported that a 6-fold increase in ionizing radiation exposure to the U.S.

population from medical procedures since the early 1980s (3), in particular finding that 10.5% of the entire radiation burden was related to MPI (4).

Owing to these considerations, professional societies have developed appropriate use criteria for MPI in order to lower its radiation dose and costs (5-7). Correspondingly, vendors have developed dedicated cardiac SPECT scanners with solid-state semiconductor detectors, primarily to address the concerns about radiation dose and long imaging time. In this review, we will focus on the latest advances in MPI procedures which ought to be able to maximize the value of state-of-art cardiac SPECT scanners with semiconductor detectors in the current era demanding reduced costs, examination time, and radiation exposure.

doi : 10.17996/ANC.01.01.18

1) Masao Miyagawa, Yoshiko Nishiyama, Rami Tashiro, Hayato Ishimura, Teruhito Mochizuki
Department of Radiology, Ehime University Graduate School of Medicine, Shitsukawa, Toon-city, Ehime, Japan, 791-0295
E-mail: miyagawa@m.ehime-u.ac.jp

2) Yasuyuki Takahashi
Department of Nuclear Medicine Technology, Gunma Prefectural College of Health Sciences.

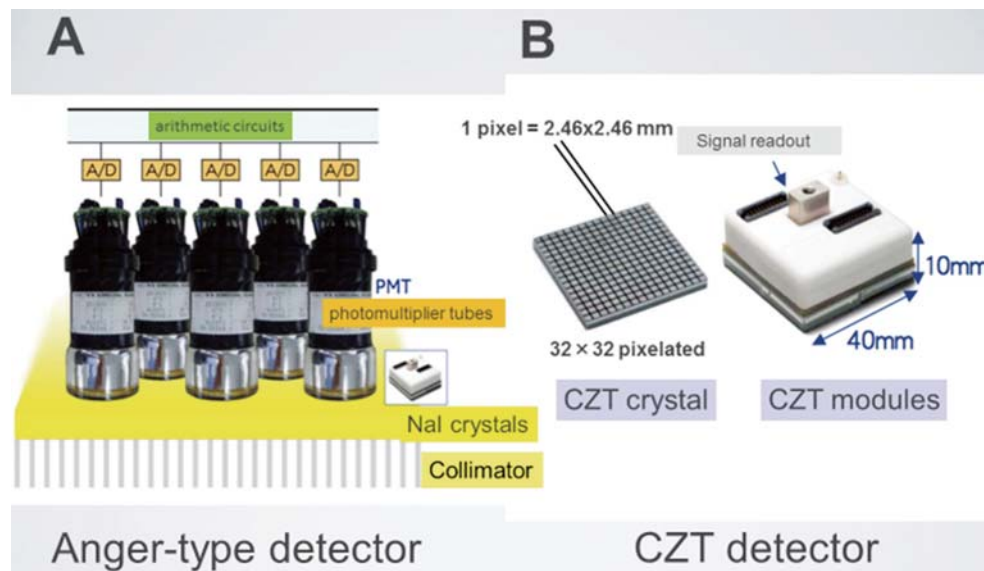


Fig. 1 Comparison of 2 different detectors

A: A 4 × 4 cm CZT detector module has a compact size as compared to the combination of NaI crystals with photomultiplier tubes of the conventional Anger camera.

B: Each detector contained 32 × 32 pixelated CZT elements (1024 elements with thickness of 2.46 × 2.46 × 5 mm). CZT = Cadmium Zinc Telluride, NaI = sodium iodide



Fig. 2 An ultra-fast cardiac SPECT camera (Discovery NM530c)

A gantry that is similar to a conventional cardiac SPECT camera, with a different detector assembly that is completely stationary during acquisition.

Technological advantages of cardiac SPECT with semiconductor detectors

Conventional SPECT is typically performed using an Anger scintillation camera, which is based on a design advanced by Berkeley electrical engineer Hal Anger in 1957 (8). Typically, each scintillation camera is equipped with parallel-hole high-resolution collimators. Since collimation is necessary to acquire the projection views, less than 0.02% of the photons emitted from the heart

are collected (9). As a result, acquisition times of 15–20 min are required for myocardial SPECT studies.

Recently, two vendors have introduced novel scanners: Discovery NM530c (D530c); GE Healthcare and D-SPECT; Spectrum Dynamics utilizing the same cadmium zinc-telluride (CZT) detectors (Fig. 1), with a different combination of high-sensitivity multi-pinhole (Fig. 2–4) or parallel-hole collimator which focuses on the myocardium (10,11). More than 300 of

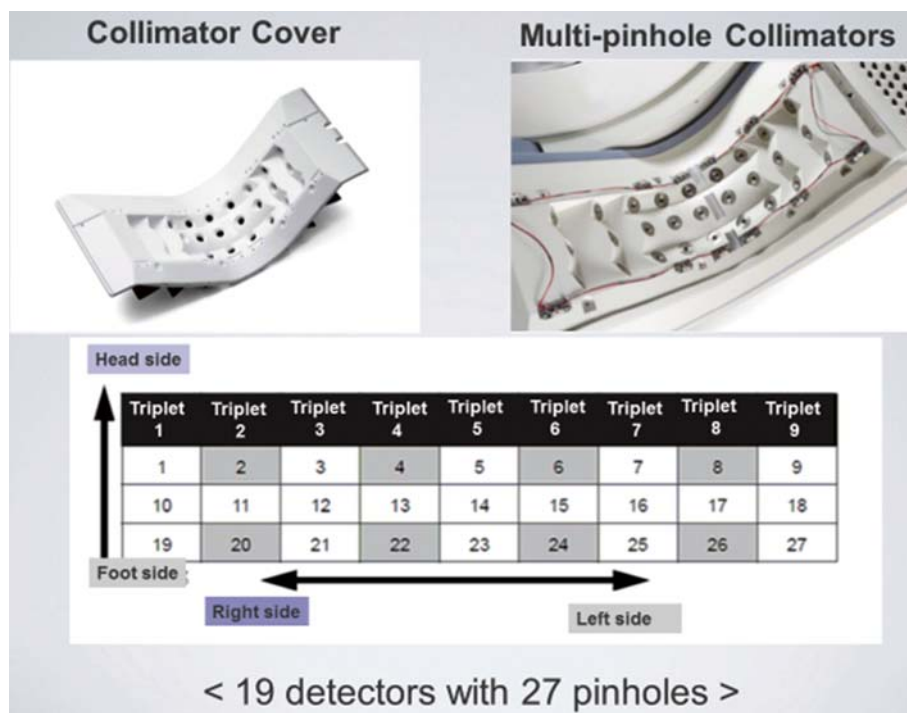


Fig. 3 Multi-pinhole Collimators

There are 9 triplets with 27 pinholes. Nineteen CZT detectors are allocated to the pinhole numbers of 1, 3, 5, 7, 9-19, 21, 23, 25, 27, respectively. There are no CZT detector in the pinholes which are shown as 10 gray areas.

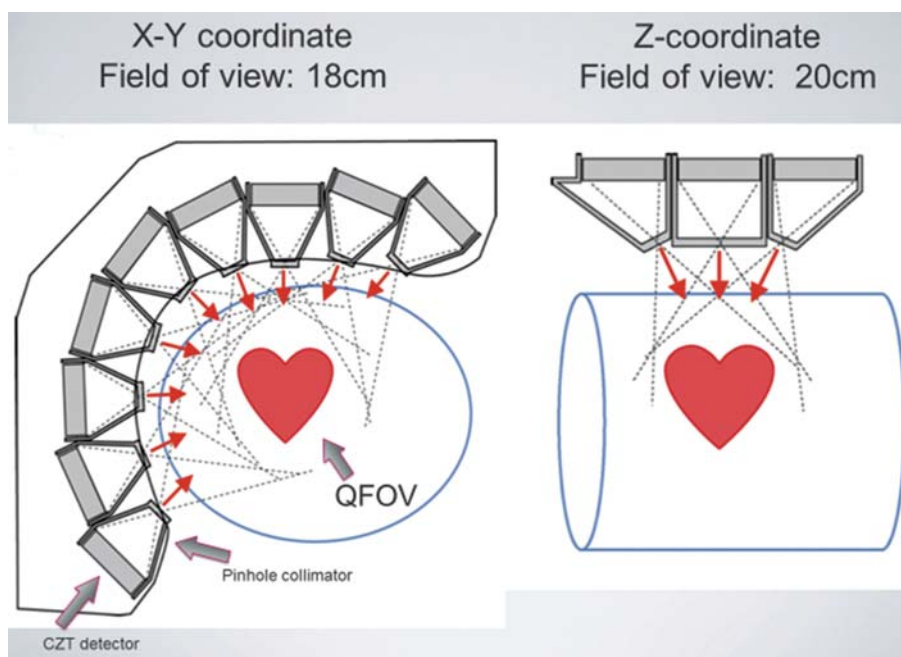


Fig. 4 A curved array of solid-state CZT detectors with optimal geometry

The detector heads are directed to the heart and the region around it. The target volume for high quality imaging is called quality field of view (QFOV) which is approximately a sphere of 18 cm diameter

such cardiac CZT SPECT scanners are currently available in the world, and the number is increasing by more than 100 per year.

We conducted a comparative study using ^{99m}Tc line-

source phantoms with and without photon scattering caused by water in the cylinder (12). D530c had a higher spatial resolution than did the conventional Anger camera with a NaI scintillation crystal and a

Table 1 FWHM by three ^{99m}Tc line sources

	Without water	With water
D530c		
Central	3.00	6.64
Tangential	3.48	5.03
Radial	1.73	3.88
Infinia		
Central	11.05	15.48
Tangential	12.63	16.28
Radial	8.17	15.61

unit; mm

dual-detector (Infinia; GE Healthcare). The measured FWHM values are summarized in Table 1. We also found that a D530c has better energy resolution compared to Infinia, which is as narrow as 5%. Therefore, energy window width could be narrowed enough to be feasible for performing dual radioisotope simultaneous SPECT with ^{99m}Tc -tetrofosmin and ^{123}I -BMIPP (13). Moreover, the high sensitivity of D530c allows for a shorter acquisition time, actually, 5 min is sufficient for QGS in the clinical setting. Although CZT detectors are higher in cost, they have been shown to provide an 8- to 10-fold increase in sensitivity, coupled with a 2-fold improvement in spatial resolution, and higher energy resolution enabling a significant reduction in imaging time and dose of isotopes, and a dual radionuclide simultaneous SPECT with ^{99m}Tc and ^{123}I (10, 11). Imbert et al. also conducted analyses of phantom and human SPECT images, comparing the D530c and D-SPECT CZT cameras with Anger cameras and reported that the physical performance of CZT cameras is dramatically higher than that of Anger cameras, however, 2 CZT cameras are inherently different. Spatial resolution and contrast-to-noise ratio are better with the Discovery NM 530c, whereas detection sensitivity is markedly higher with the D-SPECT (14).

Optimal imaging protocol for CZT SPECT

Reduction in injection dose of radiopharmaceuticals

The introduction of CZT cameras has opened the possibility of reducing radiation dose of SPECT MPI. Oddstig et al (15), reported that they performed a 1-day ^{99m}Tc -tetrofosmin stress-rest protocol using D530c in 150 patients who were divided into three subgroups (50 patients in each group) with 4, 3, and 2.5 MBq/kg body weight of administered activity in the stress MPI, respectively. The total effective dose (stress and rest) decreased from 9.3 mSv in the 4 MBq/kg group to 5.8 mSv in the 2.5 MBq/kg group.

The image acquisition times for 2.5 MBq/kg were 8 and 5 minutes (stress and rest, respectively) compared to 15 minutes for each when using conventional SPECT. The average image quality for the stress and the rest showed no statistically significant difference among the 4, 3, and 2.5 MBq/kg groups. Starting the MPS protocol with examination at stress and analyzing the stress images before deciding of the need for rest examination (that is to say "stress only protocol") reduce the effective dose. The effective dose was no more than 1.4 mSv for a patient receiving 2.5 MBq/kg, who underwent the stress only protocol. A protocol for CZT SPECT in our institution is shown in Fig. 5. The total effective radiation dose ranged 3.4 to 6.7 mSv. Novel CZT technology can considerably decrease the effective dose and acquisition time for MPI with preserved high image quality.

Stress only protocol

A strategy of the stress only protocol has reduced the effective dose and offered higher laboratory throughput. Duvall et al. reported that over 4,000 patients with more than 50% undergoing the stress only protocol successfully in an Emergency Department Chest Pain Unit. The return rate for rest imaging in the group of the stress only protocol was very low at 5% (16). There are technical matters for abnormal stress images such as soft tissue attenuation or patient motion. The return rate for rest imaging without attenuation correction and QGS analysis has been reported to be more than 50%, which would limit the benefit of performing a stress only protocol.

As an alternative to attenuation correction, accuracy could also be improved with images which were obtained by using supine-prone (Fig. 5) or supine-upright positions (17,18). Goto et al. reported that 322 consecutive Japanese patients with a high pretest probability of CAD, experienced a 1-day ^{99m}Tc -tetrofosmin stress and rest MPI by the D530c camera, and also coronary angiography (19). Of 124 patients with inferolateral perfusion defect on supine stress imaging, immediately thereafter, 63 (51%) were judged to be normal on prone imaging. They found that the overall return rate for rest imaging was 19% with combined stress supine and prone imaging, which was lower than 39% with the supine imaging alone in detection of inferolateral CAD. Consequently, the majority of patients (97%) with normal supine and prone imaging did not have angiography-confirmed CAD. In a similar study with 748 patients who had significantly larger body mass indexes than the Japanese population,

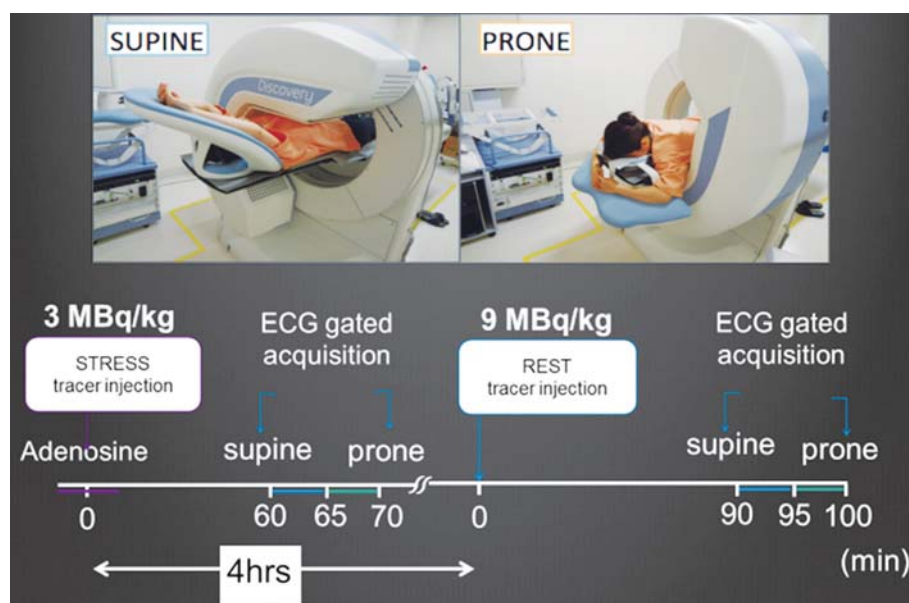


Fig. 5 Imaging protocol of our institution for CZT SPECT

We adopt a stress/rest one-day protocol with ^{99m}Tc -perfusion radiotracers. Supine and prone positionings are routinely performed. The total effective dose ranged 3.4 to 6.7 mSv. The stress-only protocol can be performed with the effective dose averaging 1 mSv.

Worden et al. (20) demonstrated that the return rate for rest imaging was 23% with a “second look” prone stress imaging, which was lower than 64% with the supine imaging alone.

More recently, Einstein et al. (21) also performed the stress-first MPI using supine and prone positions by the D530c camera in patients with chest pain. They demonstrated that in patients who did not have a high pretest probability, stress-only imaging could be performed in more than two thirds of patients with an effective dose averaging 1 mSv. An excellent prognosis was found with only 4% of the patients presenting again to the hospital within 3 months, and no death or acute coronary syndrome at 1 year.

Imaging obese patients

Obesity may often affect the quality of conventional MPI, mainly because of decreasing test specificity by diaphragm attenuation or extra-cardiac radionuclide activity. Attenuation correction has been found to improve diagnostic accuracy. The CZT cameras were expected to offer improved image quality even in obese patients. However, Fiechter et al (22), reported poor diagnostic quality in severely obese patients with body mass index (BMI) greater than 40 kg/m^2 . In those patients, image quality was non-diagnostic in 81%, which decreased to 55% after CT-based attenuation correction. They also realized that repositioning of the patients resulted in improved image quality. They concluded the poor quality may be due to the difficult

positioning of such severely obese patients in the limited field-of-view of D530c. The volume which shows the intersection of the 19 views from each pinhole is named the quality field of view (QFOV). It is a sphere with a diameter of 18 cm in which the heart needs to be positioned correctly (Fig. 4). For most of all patients in our daily routine, whose BMI are smaller than 40 kg/m^2 , such concern does not exist (Fig. 6). However, this limitation might be critical in morbidly obese patients. And moreover, accurate positioning of the patient's heart within the center of the QFOV is very important for the D530c camera to avoid positioning related artifact (23).

Attempts to estimate of coronary flow reserve using CZT SPECT

Fractional flow reserve (FFR) has become the standard method to assess ischemic heart disease in the catheterization laboratory after the demonstration that decision-making based on FFR results in better patient outcomes than angiography-guided revascularization (24). At present, coronary flow reserve (CFR) has been mostly replaced by FFR primarily due to its technical simplicity in the catheterization lab. In contrast, in the noninvasive field, quantification of PET-derived CFR is an emerging index used for improving both the diagnosis and risk stratification in patients with suspected CAD. And with the increased use, reliable evidences have been suggested that CFR is a powerful independent predictor of cardiac events and mortality

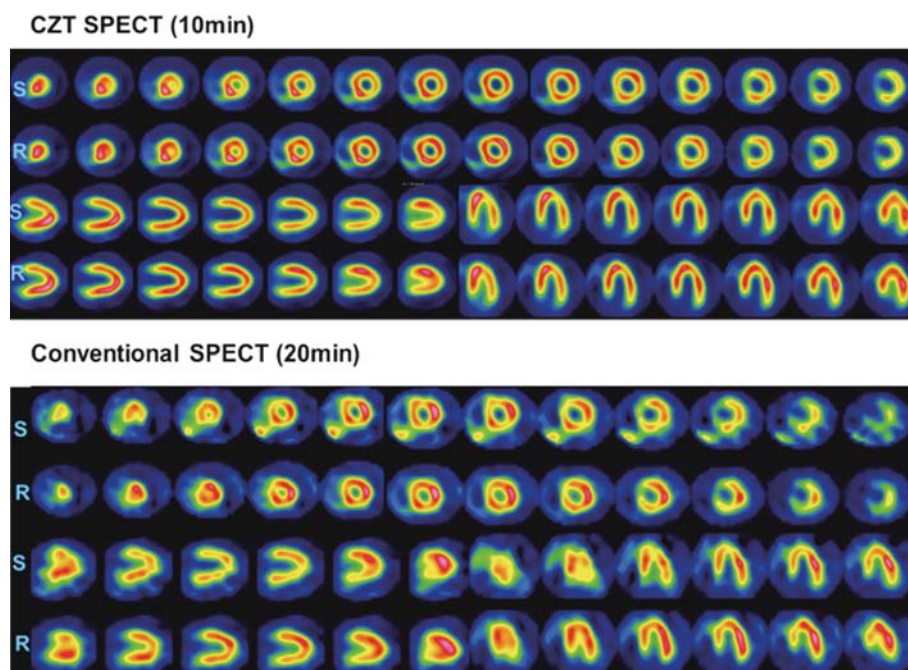


Fig. 6 Myocardial perfusion imaging of an obese patient (10 min acquisition with D530c and 20 min acquisition with Infinia)

A female patient in her 60's with chest pain, whose body weight is 93 kg (body mass index: 35.3 kg/m^2) underwent with $^{99\text{m}}\text{Tc}$ -tetrofosmin CZT SPECT imaging with D530c (upper panel), immediately followed by a conventional camera (lower panel). There are some perfusion defects probably due to attenuation artifacts in the images by a conventional camera, but no such defects are found in those by D530c. S=stress, R = rest

(25–29).

While at the same time, some studies have reported that using first-pass planar scintigraphy in humans (30–34) or dynamic SPECT in animals (35), providing evidences that the estimates of CFR can be also derived from conventional SPECT MPI. Although fair agreements have been noted between CFR estimated by SPECT and PET or intracoronary Doppler flow studies, they also highlighted the limitations of conventional gamma camera for the dynamic data collection during rapidly changing radiotracer concentrations (36).

The CZT cameras provide higher temporal and spatial resolution. Dynamic SPECT imaging during the first pass of a tracer was attained with use of these cameras. From the list data, time activity curves (TAC) would be generated for the left ventricular cavity (input function) and for myocardial tissue (output function) during stress and rest. Ben-Haim et al. (37) firstly reported the feasibility of dynamic $^{99\text{m}}\text{Tc}$ -MIBI SPECT and quantitation of global and regional CFRs using the D-SPECT. They calculated CFR index as the ratio of the stress and rest K1 values. Global CFR index was higher in patients with normal MPI than in patients with abnormal MPI. The CFR index was lower in territories supplied by stenosed coronary arteries than in non-stenosed arteries. In Fig. 7, TACs by

dynamic $^{99\text{m}}\text{Tc}$ -tetrofosmin SPECT using the D530c in our laboratory during pharmacologic stress and rest are shown. Novel software is currently under development in our institution (38).

Most recently, Wells et al. applied the D530c to a study with a pig model for quantitation of absolute myocardial blood flow (MBF) using common perfusion tracers as $^{99\text{m}}\text{Tc}$ -MIBI, $^{99\text{m}}\text{Tc}$ -tetrofosmin, and ^{201}Tl (39). Dynamic images were reconstructed with CT-based attenuation correction and energy window-based scatter correction, then processed with kinetic analysis using a 1-tissue compartment model to obtain the uptake rate constant K1 as a function of microsphere MBF. Converting K1 back to MBF using the measured extraction fractions produced accurate values and good correlations with microsphere MBF. They have demonstrated that dynamic SPECT by the CZT camera may be feasible to estimate of absolute MBF.

Advantages and disadvantages of the measurement of CFR with SPECT

At the current moment, PET plays a major role in accurate estimation of MBF or CFR. However, it has limited value for routine clinical studies because of its higher cost and more complicated procedures, including the production of short-half-lived positron tracers by

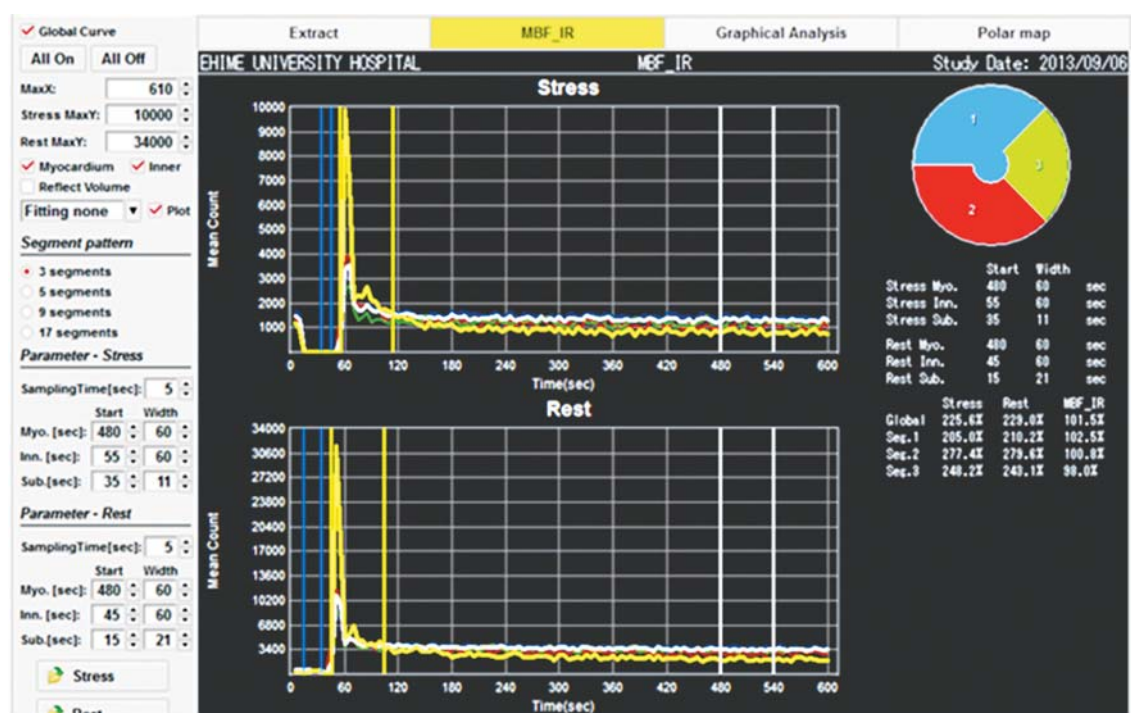


Fig. 7 Time activity curves (TAC) with ^{99m}Tc -tetrofosmin by dynamic SPECT during ATP stress and at rest

Dynamic acquisition data with list-mode were transferred to a workstation for analysis using our original software. It allows the automatic definition of a volume of interest (VOI) for the blood pool in the left ventricle and the left ventricular myocardium. The VOI-related TAC can be extracted by averaging the signal intensity in the VOI in each time frame, then, expressed in counts per mm^3/sec . Global TAC was fitted to a 2-compartment kinetic model with input functions which was served by the blood pool curves.

in-house cyclotrons. Therefore, the advantage of SPECT-measured technique utilizing common ^{99m}Tc technetium perfusion tracers, is that it would increase the utility of CFR measurement in the clinical setting with a much smaller financial cost.

On the other hand, the disadvantage of quantifying CFR with SPECT may be underestimation of the CFR value, compared to that with PET. The reasons for this underestimation could be mainly due to the limited extraction of ^{99m}Tc technetium perfusion tracers at high flow rates, at which the extraction of the tracer becomes limited by membrane transport (36).

Conclusions and future directions

Now is the time to move to a new paradigm of CZT SPECT technology. We need to explore patient centered, radiation exposure controlled, and appropriately-designed protocols which do not sacrifice image quality or diagnostic accuracy of the new modality. Although ^{99m}Tc -labeled radiotracers might not be ideal flow agents, estimation of absolute MBF or CFR using dynamic CZT SPECT is challenging and of great interest. This technology will hold great promise if the several issues can be solved through future studies.

Acknowledgments

This study was partly supported by Japan Society for Promotion of Science (JSPS), Grant-in-Aid for Scientific Research (Category C); Grant Number 25461829.

Sources of Funding

None

Conflicts of Interest

None

Reprint requests and correspondence :

Masao Miyagawa,
Department of Radiology, Ehime University Graduate
School of Medicine, Shitsukawa, Toon-city, Ehime,
Japan, 791-0295
E-mail : miyagawa@m.ehime-u.ac.jp

References

1. McNulty EJ, Hung Y, Almers LM, Go AS, Yeh RW. Population trends from 2000-2011 in nuclear myocardial perfusion imaging use. JAMA 2014; 311: 1248-9.
2. Levin DC, Rao VM, Parker L, Frangos AJ, Sunshine JH. Recent shifts in place of service for noninvasive diagnostic imaging: Have hospitals missed an opportu-

- ity? J Am Coll Radiol 2009; 6: 96-9.
3. National Council on Radiation Protection and Measurements. Report No. 160, Ionizing Radiation Exposure of the Population of the United States: National Council on Radiation Protection and Measurements; 2009.
4. Einstein AJ. Effects of radiation exposure from cardiac imaging: how good are the data? J Am Coll Cardiol 2012; 59: 553-65.
5. Hendel RC, Berman DS, Di Carli MF, et al. ACCF/ASNC/ACR/AHA/ASE/SCCT/SCMR/SNM 2009 appropriate use criteria for cardiac radionuclide imaging: a report of the American College of Cardiology Foundation Appropriate Use Criteria Task Force, the American Society of Nuclear Cardiology, the American College of Radiology, the American Heart Association, the American Society of Echocardiography, the Society of Cardiovascular Computed Tomography, the Society for Cardiovascular Magnetic Resonance, and the Society of Nuclear Medicine. Circulation 2009; 119: e561-87.
6. Cerqueira MD, Allman KC, Ficaro EP, et al. Recommendations for reducing radiation exposure in myocardial perfusion imaging. J Nucl Cardiol 2010; 17: 709-18.
7. DePuey EG, Mahmarian JJ, Miller TD, et al. Patient-centered imaging. ASNC Preferred Practice Statement. J Nucl Cardiol 2012; 19: 185-215.
8. Anger HO. Scintillation camera with multichannel collimators. J Nucl Med 1964; 5: 515-31.
9. Gambhir SS, Berman DS, Ziffer J, et al. A novel high-sensitivity rapid-acquisition single-photon cardiac imaging camera. J Nucl Med 2009; 50: 635-43.
10. Bocher M, Blevis IM, Tsukerman L, Shrem Y, Kovalski G, Volokh L. A fast cardiac gamma camera with dynamic SPECT capabilities: Design, system validation and future potential. Eur J Nucl Med Mol Imaging 2010; 37: 1887-902.
11. Patton J, Slomka P, Germano G, Berman D. Recent technologic advances in nuclear cardiology. J Nucl Cardiol 2007; 14: 501-13.
12. Takahashi Y, Miyagawa M, Nishiyama Y, Ishimura H, Mochizuki T. Performance of a semiconductor SPECT system: comparison with a conventional Anger-type SPECT instrument. Ann Nucl Med 2013; 27: 11-6.
13. Takahashi Y, Miyagawa M, Nishiyama Y, Kawaguchi N, Ishimura H, Mochizuki T. Dual radioisotopes simultaneous SPECT of ^{99m}Tc -tetrofosmin and ^{123}I -BMIPP using a semiconductor detector. Asia Oceania J Nucl Med Biol 2014; 3: 43-9.
14. Imbert L, Poussier S, Franken PR, et al. Compared performance of high-sensitivity cameras dedicated to myocardial perfusion SPECT: a comprehensive analysis of phantom and human images. J Nucl Med 2012; 53: 1897-903.
15. Oddstig J, Hedeer F, Jogi J, Carlsson M, Hindorf C, Engblom H. Reduced administered activity, reduced acquisition time, and preserved image quality for the new CZT camera. J Nucl Cardiol 2013; 20: 38-44.
16. Duvall WL, Wijetunga MN, Klein TM, et al. Stress-only Tc-99m myocardial perfusion imaging in an Emergency Department Chest Pain Unit. J Emerg Med 2011; 42: 642-50.
17. Nishiyama Y, Miyagawa M, Kawaguchi N, et al. Combined supine and prone myocardial perfusion single-photon emission computed tomography with a cadmium zinc telluride camera for detection of coronary artery disease. Circ J 2014; 78: 1169-75.
18. Nakazato R, Tamarappoo BK, Kang X, et al. Quantitative upright-supine high-speed SPECT myocardial perfusion imaging for detection of coronary artery disease: correlation with invasive coronary angiography. J Nucl Med 2010; 51: 1724-31.
19. Goto K, Takebayashi H, Kihara Y, et al. Impact of combined supine and prone myocardial perfusion imaging using an ultrafast cardiac gamma camera for detection of inferolateral coronary artery disease. Int J Cardiol 2014; 174: 313-7.
20. Worden NE, Lindower PD, Burns TL, Chatterjee K, Weiss RM. A second look with prone SPECT myocardial perfusion imaging reduces the need for angiography in patients at low risk for cardiac death or MI. Nucl Cardiol 2015; 22: 115-22.
21. Einstein AJ, Johnson LL, DeLuca AJ, et al. Radiation dose and prognosis of ultra-low-dose stress-first myocardial perfusion SPECT in patients with chest pain using a high-efficiency camera. J Nucl Med 2015; 56: 545-51.
22. Fiechter M, Gebhard C, Fuchs TA, et al. Cadmium-zinc-telluride myocardial perfusion imaging in obese patients. J Nucl Med 2012; 53: 1401-6.
23. Hindorf C, Oddstig J, Hedeer F, Hansson MJ, Jögi J, Engblom H. Importance of correct patient positioning in myocardial perfusion SPECT when using a CZT camera. J Nucl Cardiol 2014; 21: 695-702.
24. van de Hoef TP, Meuwissen M, Escaned J, et al. Fractional flow reserve as a surrogate for inducible myocardial ischaemia. Nat Rev Cardiol 2013; 10: 439-52.
25. Yoshinaga K, Chow BJ, Williams K, et al. What is the prognostic value of myocardial perfusion imaging using rubidium-82 positron emission tomography? J Am Coll Cardiol 2006; 48: 1029-39.
26. Herzog BA, Husmann L, Valenta I, et al. Long-term prognostic value of ^{13}N ammonia myocardial perfusion positron emission tomography added value of coronary flow reserve. J Am Coll Cardiol 2009; 54: 150-6.
27. Murthy VL, Naya M, Foster CR, et al. Improved cardiac risk assessment with noninvasive measures of coronary flow reserve. Circulation 2011; 124: 2215-24.
28. Murthy VL, Naya M, Foster CR, et al. Association between coronary vascular dysfunction and cardiac mortality in patients with and without diabetes mellitus. Circulation 2012; 126: 1858-68.
29. Naya M, Murthy VL, Taqueti VR, et al. Preserved coronary flow reserve effectively excludes high-risk

- coronary artery disease on angiography. *J Nucl Med* 2014; 55: 248-55.
30. Taki J, Fujino S, Nakajima K, et al. Tc-99m retention characteristics during pharmacological hyperemia in human myocardium: comparison with coronary flow reserve measured by Doppler flowwire. *J Nucl Med* 2001; 42: 1457-63.
 31. Sugihara H, Yonekura Y, Kataoka K, Fukai D, Kitamura N, Taniguchi Y. Estimation of coronary flow reserve with the use of dynamic planar and SPECT images of Tc-99m tetrofosmin. *J Nucl Cardiol* 2001; 8: 575-9.
 32. Ito Y, Katoh C, Noriyasu K, et al. Estimation of myocardial blood flow and myocardial flow reserve by ^{99m}Tc-sestamibi imaging: comparison with the results of O-15 H₂O PET. *Eur J Nucl Med Mol Imaging* 2003; 30: 281-7.
 33. Storto G, Cirillo P, Vicario ML, et al. Estimation of coronary flow reserve by Tc-99m sestamibi imaging in patients with coronary artery disease: comparison with the results of intracoronary Doppler technique. *J Nucl Cardiol* 2004; 11: 682-8.
 34. Daniele S, Nappi C, Acampa W, et al. Incremental prognostic value of coronary flow reserve assessed with single-photon emission computed tomography. *J Nucl Cardiol* 2011; 18: 612-9.
 35. Iida H, Eberl S, Kim KM, et al. Absolute quantitation of myocardial blood flow with ²⁰¹Tl and dynamic SPECT in canine: optimization and validation of kinetic modeling. *Eur J Nucl Med Mol Imaging* 2008; 35: 896-905.
 36. Petretta M, Soricelli A, Storto G, Cuocolo A. Assessment of coronary flow reserve using single photon emission computed tomography with technetium 99m-labeled tracers. *J Nucl Cardiol* 2008; 15: 456-65.
 37. Ben-Haim S, Murthy VL, Breault C, et al. Quantification of myocardial perfusion reserve using dynamic SPECT imaging in humans: a feasibility study. *J Nucl Med* 2013; 54: 873-9.
 38. Miyagawa M, Nishiyama Y, Kawaguchi N, et al. Estimation of myocardial flow reserve using a cadmium-zinc telluride (CZT) SPECT in patients with multi-vessel coronary artery disease. *J Nucl Med* 2013; 54: Supplement 157P.
 39. Wells RG, Timmins R, Klein R, et al. Dynamic SPECT measurement of absolute myocardial blood flow in a porcine model. *J Nucl Med* 2014; 55: 1685-91.